Site-Specific Labeling and the Distribution of Free Volume in Glassy Polystyrene

Wei-Ching Yu and Chong Sook Paik Sung*

Institute of Materials Science, Department of Chemistry, University of Connecticut, Storrs, Connecticut 06268

Richard E. Robertson*

Department of Materials Science and Engineering, The University of Michigan, Ann Arbor, Michigan 48109-2136. *Received July 1, 1987*

ABSTRACT: Free volume environments at different sites along the polystyrene molecule have been evaluated by site-specific labeling with azobenzene chromophores. The sites investigated are the regions around the chain ends, the chain sides, and the chain centers along the backbone. Also investigated was the free volume of the least constrained regions between the chains by the use of free probes not attached to the polymer molecule. Trans → cis photoisomerization kinetics of the labels and the free probe were studied at 70, 80, and 90 °C as a function of annealing time following cooling from the melt. The photoisomerization kinetics suggest that each of the labels and the free probe can find itself in one of two different environments. In one environment, accounting for a fraction α of each of the chromophores, photoisomerization was rapid; in the other environment, photoisomerization was very slow. The fractions of rapidly photoisomerizing chromophores were found to decrease with aging time, with the change being similar though not identical for each site. The magnitudes of the rapid fractions always remained in the following descending order, however: free probe, chain ends, side groups, and chain center. The Robertson–Simha–Curro (RSC) theory was used to compute the populations of regions having a greater than critical amount of free volume, and these were then compared with the experimentally measured fraction (α) of the fast photoisomerization. Except for recovery at 30 °C below the glass transition temperature, at which temperature and below the computational approach appears to be inadequate, the computed fit to the data was very satisfactory. This suggests that photoisomerizable labels and to some extent the free probe are able to ascertain the magnitude of the local free volume at various locations in bulk polymer. It suggests also that the basis of the RSC theory, involving a distribution of free volumes arising from thermal fluctuations, is correct.

Introduction

The properties of glassy polymers are known to be strongly influenced by the density of molecular packing of free volume. Such dependence on free volume is clearly manifested in the spontaneous change in behavior with time of glassy polymers that is widely known as physical aging.[1] During the course of physical aging, the enthalpy[2] and volume, and by implication the free volume, decrease with consequent embrittlement[3] and decrease in gas permeability.[4] Although the free volume concept has been very useful in explaining the overall behavior of glassy polymers in regard to volume recovery and other macroscopic properties, it is insufficient for explaining other important features of glassy polymers. For example, the creep behavior of polystyrene at 93 °C continues to change even after the enthalpy, and presumably free volume, have reached constant values,[5] and similarly, the thermal density fluctuations considerably lag the approach to equilibrium of the volume.[6] A possible solution is to invoke along with the overall free volume the idea of the size distribution of free volume and its change with time, temperature, and pressure. This concept has already received theoretical consideration.[7] Since amorphous polymers lack structural order, the distribution of free volume may be the best way to characterize them.

The purpose of the work described herein has been to evaluate the free volume environments at different sites along the polymer molecule. The sites investigated are the regions around the chain ends, the chain sides, and the chain centers along the backbone. The regions around the chain ends, for instance, have been traditionally thought to contain more free volume than the rest of the chain, thus accounting for the dependence of the glass transition temperature on the molecular weight. Also investigated was the free volume between the chains, probably the least constrained regions between the chains, by the use of free probes not attached to the polymer molecule. Besides the general free volume at different sites in the polymer, the change with time of these free volumes during physical aging has also been studied. A further purpose of this work has been to test the fundamental assumption of the free volume distribution used in the theory of one of us for structural recovery or physical aging.[8]

Different techniques have been used to estimate free volume sizes in glassy polymers. Small-angle X-ray scattering (SAXS) has been extensively used by Roe et al. to determine density fluctuations and thus to obtain a measure of a free volume size distribution.[6b,9] Roe et al. found that density fluctuations were more sensitive than were the specific volume to isothermal annealing, rate of cooling, pressure-release, and the changing of molecular weight.[9a] This sensitivity has been discussed by Jain and Simha.[7d] From density fluctuation data, Roe et al. estimated the weight-average size of the holes in poly(methyl methacrylate) based on a simple model of random distribution of free volume sizes, to have a volume of 105 Å.[9b]

Positronium annihilation spectroscopy (PAS) provides estimates of average free volume sizes by monitoring the lifetimes of positron species, which depend strongly on the electron density of the environment.[10] Specifically, the lifetime of triplet state positronium atom increases when the dimensions of free volume holes increases due to reduced overlap with the atom. Using calibration curves to relate free volume sizes to triplet positronium atom lifetimes in simple van der Waals-bonded molecules,[11] Jean et al. estimated the hole sizes to vary with temperature from 25 to 222 Å^3 in glassy epoxy matrix.[12] For thermoplastic glassy polymers, Malhorta and Pethrick, following the analysis of Ujihara et al.,[13] estimated the hole sizes to be between 20 and 70 Å^3 in polycarbonate, polysulfone, and polyether sulfone.[14]

Recently, we demonstrated that photochromic labels attached to polymer molecules can be used to probe free volume and its size distribution in glassy polymers.[15] By

0024-9297/88/2221-0355$01.50/0

the analyses of the photoisomerization behavior of photochromic labels, such processes as physical aging, plasticization, and volume dilation due to tensile deformation have been sensitively monitored. While photoisomerization of the attached label is characterized by a single rate constant in dilute solution, at least two rates have to be invoked for the solid. The fast rate is similar to the rate in dilute solution, and the slow rate is at least 100 times slower. The fraction (α) of the fast process decreases with physical aging but increases with temperature, plasticization, or deformation. Under the assumption that photoisomerization requires a critical free volume in the immediate vicinity of the label, we interpreted the fast fraction, α, to be the cumulative area under the free volume distribution curve for free volumes above the critical size for the particular label. Such bimodal features (fast and slow motions) had been also observed by ESR spin probe and label studies in glassy polymers.[16]

In our earlier study, the photochromic azo labels were attached randomly to the polymer main chains.[15] In this study, we report on the physical aging studies on polystyrenes labeled at three specific chain sites, namely, the chain center, the chain end, or the side group. The photoisomerization behavior of these site-specific labeled polymers was studied in the earlier work at 20 °C.[17] In dilute solution, only a small difference in the photoisomerization behavior was found at different sites of the chain. However, a much greater difference was observed at 20 °C in the glassy state; only 8% of the center label was found to photoisomerize while about 45% of the chain end of the side group could do so. Physical aging is too slow to be monitored at 20 °C. In order to measure physical aging within reasonable time scale, we aged polymers at 10, 20, and 30 °C below T_g following a temperature jump from 10 or 20 °C above T_g in the present study. Also, the behavior of the labels will be compared with that of the probe molecule which is merely dispersed in small concentration throughout the polystyrene matrix. In studies involving free probes, an implicit assumption is usually made that the probe represents the average free volume environment. We are particularly interested in testing this assumption by comparing the site-specific labels and the free probe.

Finally, we compare the resulting experimental data with theoretical predictions based on the kinetic theory of Robertson, Simha, and Curro (RSC theory).[18] The summary of this theory will be described following the Experimental Procedures.

Experimental Procedures

Materials. The syntheses and purification of labeled polystyrenes was described in our earlier paper.[17] Chart I provides chemical structures and some characteristics of the labeled polymers. A free probe molecule, *p*-aminoazobenzene from Eastman Kodak Chemical, was recrystallized from toluene and acetone. The free probe (1 mg) was dissolved in 25 mL of benzene with 2.5 g of polystyrene (MW 80 000 from Pressure Chemical Co.). This corresponds to a concentration of 2.03×10^{-3} M. At this concentration, it is known that no aggregation of the free probe occurs,[19] and we confirmed molecular dispersion by comparing UV–vis absorption spectra of the probe in bulk polystyrene with that in dilute benzene solution. Films from the labeled polystyrene solutions (7–10% by wt) or from free probe-containing polystyrene solution were obtained by casting on quartz plates at room temperature, followed by a careful, slow drying in a vacuum oven at room temperature to prevent the formation of bubbles. The vacuum and temperature of the vacuum oven were raised slowly to ≈3 Torr and ≈125 °C, respectively, in five stages in 1 day. Then, the samples were kept at this temperature for 2 days to completely remove the solvent.

Photoisomerization Studies. The prepared films on the quartz plates were annealed at 110 or 120 °C for 2 h to reach equilibrium and then cooled to a specific temperature (70, 80, or 90 °C), followed by aging for different periods of time. The aged samples were taken out and quenched on a metal plate to room temperature prior to photoisomerization measurements. This cooling to room temperature was necessary because the thermal back reaction at the aging temperatures is too fast to allow accurate measurements. A PRS flash light source (Model 6100A) was used to irradiate the sample to cause trans → cis photoisomerization. UV–visible spectra of the sample were taken with a Perkin-Elmer diode-array system with a Model 7500 data station right after a certain number of flashes had irradiated it. The sample was fixed at 45 °C to the analyzed beam and at 135 °C to the irradiating beam to obtain accurate readings. The labeled polystyrenes and the free *p*-aminoazobenzene were dissolved in benzene for photoisomerization studies in dilute solutions. The solution sample in a quartz cell (fluorescence cuvette) was positioned at the intersection point of the analyzed beam and the irradiating beam. The initial optical densities of trans isomer absorption peaks in film and solution samples were in the range of 0.6–1.1. To prevent the interference from random luminescence, the measurements were performed in a dark room.

Theory

The association between the kinetics of molecular processes in condensed phases and "free volume" is so intuitive as to be obvious. Not so obvious is what measure of free volume to use; it needs to represent the local molecular packing density and fluctuations in the density in the context of the nature of the kinetic process being studied. In the following we will use the free volume derived from the Simha–Somcynsky theory for the equation of state.[20] The Simha–Somcynsky theory has been very successful in describing the pressure–temperature–volume relationships of polymer liquids.[21]

The Simha–Somcynsky theory is based on a cell model. At any finite temperature, not all of the cells are occupied. The free volume for the equilibrium liquid is set equal to the fraction of unoccupied cells obtained by minimizing the Helmholtz free energy given by the theory. When the polymer is not in an equilibrium state, as in the glass, the fraction of unoccupied cells can no longer be obtained by minimizing the Helmholtz free energy. Instead, and as an approximation, we assume that the fraction of unoccupied cells is that value that causes the volume in the theory to be the same as the measured volume.

To compute the changes in free volume during aging, it is necessary to examine changes occurring locally in the specimen. Local changes are expected to occur at rates that depend on the local free volume, and this is expected to vary throughout the specimen because of the ever-present thermal fluctuations. The importance of thermal fluctuations here arises from the very small size of the regions expected to control the kinetics of isomerization. The small size of the regions means that the breadth of the free volume distribution is large compared to the free volume average. The following is a summary of the theory, denoted by RSC, to be employed. The details are given in ref 18.

Although there is a continuous distribution of fractional free volume existing within the regions of interest, the cells within which the isomerization occurs, the computation of the changes of free volume within these cells is more easily performed for a discrete distribution. Thus, the cells are assumed to contain only certain well-defined amounts of free volume, which are assumed to be multiples of a quantity denoted by β. These discrete amounts equal to multiples of β therefore represent a set of "free volume states".

The fraction of cells that have at time t the free volume $(j-1)\beta$ are denoted by $w_j(t)$. The index j, which describes the set of free volume states, runs from 1 to n. The upper

limit n is set high enough so that almost no regions would have a free volume greater than $(n-1)\beta$. The computation of the progress of structural recovery involves computing the changes in the free volume distribution or the w_j's with time.

At equilibrium, the free volume distribution is expected to be roughly Gaussian, except that the free volume cannot assume negative values. A discrete distribution function for a nonnegative variate that can reflect this behavior is the binomial distribution. The binomial distribution has two parameters: the number of states n and the unit probability p_r. The unit probability p_r and the free volume increment β are fixed by demanding that the binomial distribution yield the average free volume and the mean square fluctuation from the average obtained from the Simha–Somcynski equation:

$$(n-1)p_r\beta = \langle f \rangle$$
$$(n-1)p_r(1-p_r)\beta^2 = \langle \delta f^2 \rangle \quad (1)$$

The state occupancies given by the binomial distribution are

$$\xi_j = \binom{n-1}{j-1} p_r^{j-1}(1-p_r)^{n-j} \quad (2)$$

For an equilibrium state, or approximately for a nonequilibrium state resulting from a sudden step in temperature or pressure applied to an equilibrium state, we have $w_j = \xi_j$.

The transitions among the various free volume states since an earlier time t_0 represents a stochastic process, depending on Brownian motion, and can be described formally by the following set of n equations[22]

$$w_j(t) = \sum_{i=1}^{n} w_i(t_0) P_{ij}(t - t_0) \quad (3)$$

where $P_{ij}(t-t_0)$ is the probability that any given region in state i at t_0 will change to state j during the time interval from t_0 to t. If the transition between any pair of states is assumed to pass through all of the intervening states, then over an infinitesimal time interval h, the transition probabilities for a state i become, approximately

$$P_{i,i-1}(h) = h\lambda_i^-$$
$$P_{i,i+1}(h) = h\lambda_i^+ \quad (4)$$
$$P_{ii}(h) = 1 - h(\lambda_i^- + \lambda_i^+)$$

with all other P_{ij}'s approximately equal to zero, where λ_i^+ and λ_i^- are the upward and downward transition rates from state i, respectively. Because the transition probabilities behave according to the following Chapman–Kolmogorov equation[22]

$$P_{ij}(t+h) = \sum_{k=1}^{n} P_{ik}(t) P_{kj}(h) \quad (5)$$

the time derivative of this equation with respect to h yields a set of coupled differential equations, which can be written in matrix form as

$$\dot{P}(t) = P(t)\cdot\mathbf{A} \quad (6)$$

where $\mathbf{A}$ is a tridiagonal matrix with $A_{ii} = -(\lambda_i^- + \lambda_i^+)$, $A_{i,i-1} = \lambda_i^-$, and $A_{i,i+1} = \lambda_i^+$ (except for $i = 1$ and n, where transitions outside the range of i are not allowed).

The upward and downward transition rates are not independent but are linked at equilibrium by the requirements of detailed balancing:

$$\xi_i\lambda_i^+ = \xi_{i+1}\lambda_{i+1}^- \quad (7)$$

The transition rates are expected to depend on the local free volume. Thus, the transition rate out of state i will be a function of the free volume $(i-1)\beta$, for example. In addition, the rates are expected to depend on the free volume of the immediately adjacent region. This is because the surrounding region must act as the source and sink for changes in free volume. The form of the volume dependence in the statistical mechanical equation for fluctuations indicates that there is no correlation between fluctuations in neighboring regions. As a result, the free volume of the immediately surrounding region will be equal on average to the global average free volume and will be independent of the free volume of the central region. The free volume affecting the transition rates out of a state i can be described, then, by[18a]

$$\hat{f}_i = [(i-1)\beta + (z-1)\langle f \rangle]/z \quad (8)$$

where $(z-1)/z$ is the volume fraction of the surrounding region that affects the kinetics of a local change of free volume by acting as a source or sink. Since the environment consists essentially of nearest neighbors, z has a value of the order of 10 or more.

The local transition rates are assumed to depend on the local free volume in the same way that the global kinetics depend on the global free volume. For this purpose, we express the WLF (Williams–Landel–Ferry) or the Vogel equation in terms of free volume instead of temperature. Because of a near linear relationship between temperature and f, the free volume given by the Simha–Somcynsky equation, the following substitution is made in the WLF and Vogel equations

$$T - T_g = (f - f_g)T^*/f^* \quad (9)$$

where f^* is defined by this equation and is obtained from plots of the free volume of the liquid above the glass transition vs temperature at constant pressure. Note that this substitution in the empirically derived WLF and Vogel equations involves no assumptions other than that there exists a linear correspondence between T and f in the equilibrium liquid state. The assumption to be made, however, is that the WLF and Vogel equations, when expressed in terms of free volume instead of temperature, can be used to represent local transition rates when the system is away from global equilibrium.

Using the Vogel form of the rate equation, the rate for the downward step in local free volume is written as

$$\lambda_i^- = R\tau_g^{-1}(\xi_{i-1}/\xi_i)^{1/2}\beta^{-2}\exp(2.303c_1[1 + c_2/(c_2 + T^*(\hat{f}_i - f_g)/f^*)]) \quad (10)$$

The rate for the upward step is obtained by combining eq 7 and 10. τ_g is the relaxation time at the glass transition. R is an adjustable parameter that remains constant for any set of data. R acts to translate from microscopic to macroscopic processes and also to compensate for inexact or uncertain values of τ_g. The factor $(\xi_{i-1}/\xi_i)^{1/2}$ in eq 10, taken out of R, allows the rates for the upward and downward steps to have the same form. The factor β^{-2} removes the free volume step size from the overall kinetics.

The formal solution to the differential equation in eq 7 is

$$P(t) = P(0)\exp(At) \quad (11)$$

To obtain a more explicit form for the solution, the eigenvalues of A need to be found. It is convenient to first symmetrize A. By applying a similarity transformation

with a diagonal matrix γ, the symmetrical matrix $\mathbf{Z} = \gamma^{-1}A\gamma$ is obtained, where

$$\gamma_i = \xi_i^{-1/2} \tag{12}$$

In terms of the eigenvalues ζ_k and the corresponding eigenvectors Q_k of the matrix $\mathbf{Z}$, the free volume state populations develop in time according to

$$w_i(t) = \sum_{k=1}^{n} \gamma_i^{-1} Q_{ik} [\sum_{j=1}^{n} w_j(t_0)\gamma_j Q_{jk}] \exp[\zeta_k(t - t_0)] \tag{13}$$

Because the eigenvalues ζ_k for $k = 1, ..., n$ are all negative, the right-hand side of eq 13 is equivalent to a sum of decaying exponentials. But the changes in the populations w_i are not quite describable by a parallel array of Maxwell models, for example. Because of the dependence given in eq 8 of $\hat{f}_i$ on the average free volume, which continuously changes during recovery, the values of the parameters in eq 13 are continuously changing also and need to be continually reevaluated in the calculation. The average free volume is given by

$$\langle f(t) \rangle = \sum_{j=2}^{n} (j - 1)\beta w_j(t) \tag{14}$$

For predicting the kinetics of isomerization, we will want to follow the changes in the population of sites having free volume both above and below some fixed, critical free volume. We will denote this critical free volume by j^*, meaning that it falls between $(j^* - 1)\beta$ and $j^*\beta$. The populations above the critical free volume is given by

$$\alpha = 1 - \sum_{j=1}^{j^*} w_j(t) \tag{15}$$

with the remainder of the population below.

Experimental Results

Photoisomerization in Dilute Solution. In an earlier study, we reported on the photoisomerization of three labeled polystyrenes in dilute benzene solution by pulsed laser spectroscopic techniques, using an intense nanosecond laser pulse (351 nm, 10 mJ, 3 ns, and operated at 5 pps).[17] In this study, physical aging studies are carried out by using a flash lamp that delivers 10-ms flashes of much less intensity as the irradiation source. Interference filters were used to match the irradiation wavelength band (~10 nm) with the absorption maximum of each label or probe. Also, in this study, we can obtain a full UV–vis spectra between flashes due to the fast diode-array detection system, while in the laser study we were only able to observe the changes in absorbance at a fixed wavelength. In view of these differences in the experimental setup, we also carried out photoisomerization studies in dilute solution, to provide base-line data for the physical aging studies.

Figures 1a, 2a, 3a, and 4a illustrate the representative UV–vis spectra as a function of photoisomerization in dilute benzene solution at 20 °C. They represent the end label, the side label, the center label, and the free probe, respectively. The free probe solution (concentration $\approx 5 \times 10^{-5}$ M) does not contain any polystyrene. Before irradiation, the absorption maximum for the trans isomer is found at 353 nm for the end and side labels, 375 nm for the center label, and 377 nm for the free probe. With increasing irradiation, as indicated by the number of flashes, the trans isomer absorption peak decreases sharply, followed by the increase in the cis isomer absorption peak at 325 nm. The extinction coefficient at 445 nm due to the $n \rightarrow \pi^*$ transition of the azo bond is greater for the cis than for the trans isomer. As a consequence, the absorption at 445 nm increases with irradiation. For the

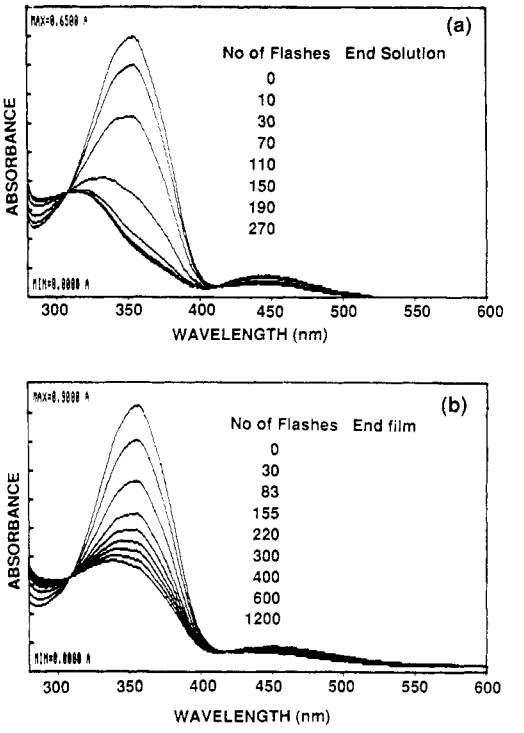

Figure 1. UV–vis absorption spectra of azobenzene end group in chain end-labeled polystyrene as a function of number of irradiating flashes at 25 °C (top, in dilute benzene solution; bottom, in the quenched (from 110 °C) glassy film).

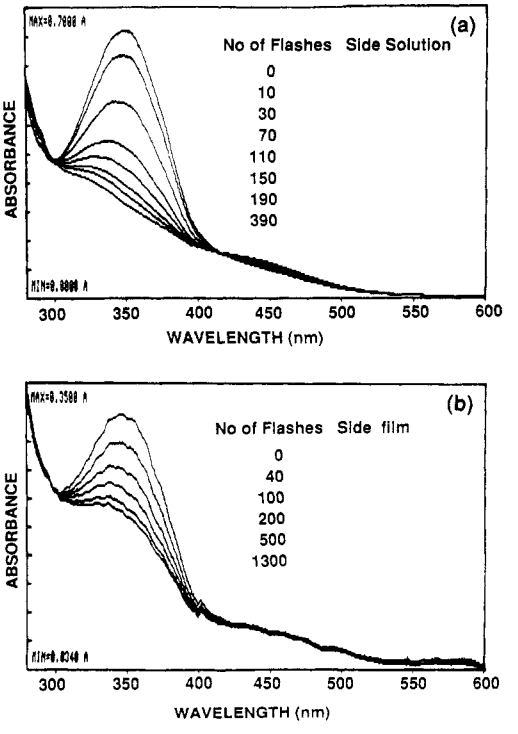

Figure 2. UV–vis absorption spectra of azobenzene side group in side chain-labeled polystyrene as a function of number of irradiating flashes at 25 °C (top, in dilute benzene solution; bottom, in the quenched (from 120 °C) glassy film).

center label and free probe, the cis isomer peak at 325 nm is fairly well separated from the trans isomer peak. For the side and end labels, the two peaks are close to each other, resulting in the two peaks overlapping. This makes the estimation of the photostationary composition difficult. But for the center label and the free probe, subtraction of the cis peaks at 325 and 425 nm from the trans peak allows us to estimate the cis isomer concentration to be

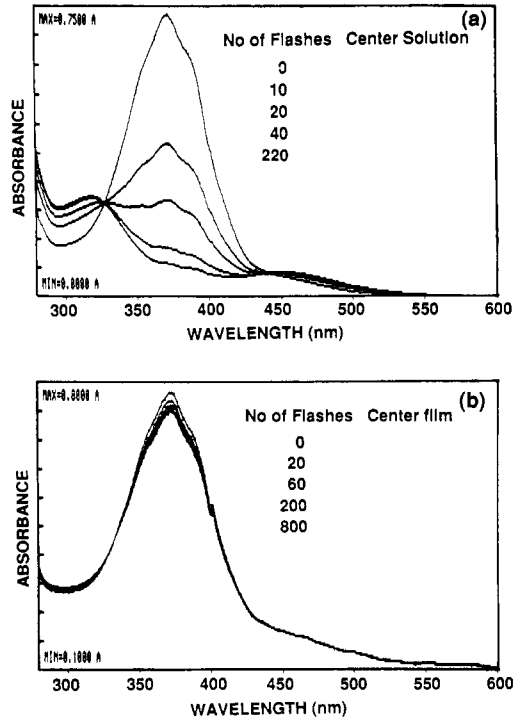

Figure 3. UV–vis absorption spectra of azobenzene chain center in the chain-center labeled polystyrene as a function of number of irradiating flashes at 25 °C (top, in dilute benzene solution; bottom, in the quenched (from 150 °C) glassy film).

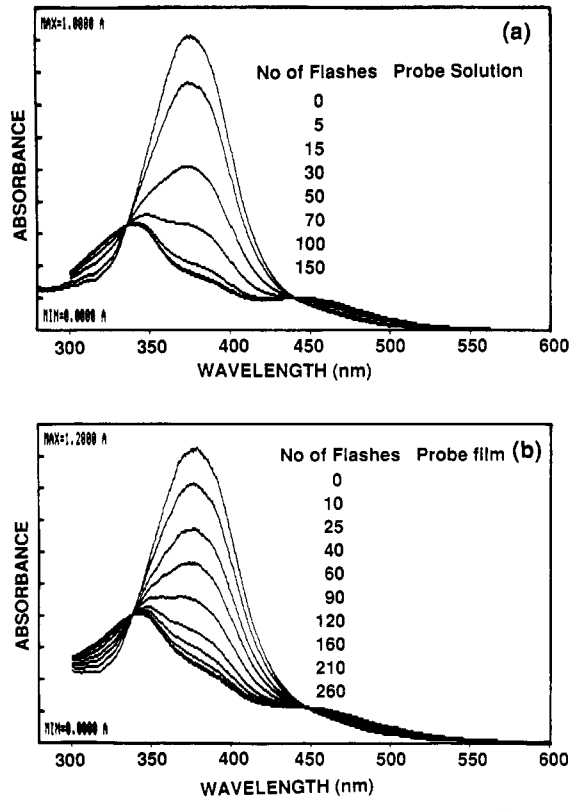

Figure 4. UV–vis absorption spectra of p-amino azobenzene as a function of number of irradiating flashes at 25 °C (top, in dilute benzene solution; bottom, in a quenched (from 110 °C) polystyrene film).

90% at the photostationary state. For the end and side labels, the cis isomer content at the photostationary state can be estimated to be about 90%, after subtraction of the cis peak. These values are larger than our previously reported values, assuming negligible cis intensity at the λ_{max} of the trans isomer.[17] For the present kinetic analyses of

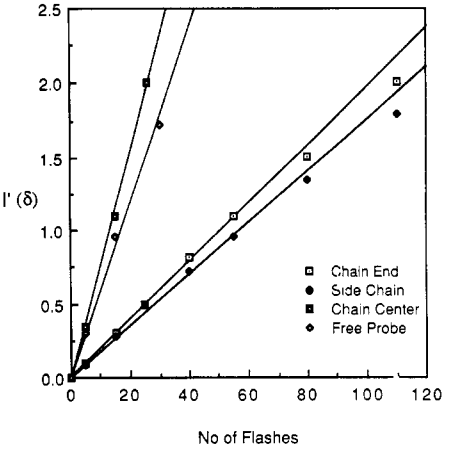

Figure 5. Kinetic plot of photoisomerization of the azobenzene labeled polystyrene and the free probe in dilute benzene solution.

Table I
Photoisomerization Parameters of Three Labeled Polystyrenes and the Probe in Dilute Solution

sample design	10^2A,[a] s^{-1}	$10^2A'$,[b] s^{-1}	Y_∞[c]
C-PS	7.34	6.67	0.1
E-PS	2.13	2.13	0.1
S-PS	1.85	1.85	0.1
probe	6.33	5.75	0.1

[a] A is the slope from Figure 5. [b] A' is the rate constant after correcting for the wavelength-dependent differences in I_0. [c] Y_∞ is the cis isomer content at the photostationary state.

photoisomerization, only the first 50% of the reaction has been used, to reduce the error due to the cis contribution. The following equation, a good approximate solution of the reversible photochemical rate equation, was used to analyze the kinetics of photoisomerization

$$I(\delta) = \left(1 + \frac{D_\infty}{2} + \frac{D_\infty^2}{12}\right) \ln|\delta| - \left(\frac{1}{2} + \frac{D_\infty}{6}\right)\delta + \frac{\delta^2}{24} = -At + \text{const} \quad (16)$$

where $\delta = D_\infty - D$ and D_∞ and D are optical densities at the photostationary state and after t flashes, respectively. On the basis of the fact that the cis content at the photostationary state is about 90%, D_∞ has been assumed to equal $0.1D_0$ where D_0 is the optical density for the trans isomer before irradiation. The plots of $I(\delta)$ vs t are illustrated in Figure 5. From the slopes of such plots, the quantum yield for the trans → cis photoisomerization may be obtained since $A = (I_0\phi_t\epsilon_t/y_\infty)$, where I_0 is the irradiation intensity, ϕ_t is the quantum yield of photoisomerization, ϵ_t is the molar extinction coefficient of the trans isomer, and y_∞ is the fraction of cis isomer at the photostationary state. However, due to the difficulty in measuring I_0 of short flashes accurately enough, we have not attempted to estimate the quantum yield. Instead, we will use the slopes of $I(\delta)$ vs t plots as the relative rate constants of photoisomerization. Table I summarizes such rate constants for the three labels and the free probe in dilute solution at 20 °C. As seen in the second column of Table I, the relative rates (A) appear to be greater for the center label and the free probe than for the end and side labels. This is due to wavelength-dependent fluctuations of the flash lamp intensity and the transmittance characteristics of the interference filters. After correcting for these differences, the relative rate constants (A') become closer as indicated in the third column of Table I. In the last column of Table I, we list the cis content at the photostationary state, after subtraction of the cis isomer ab-

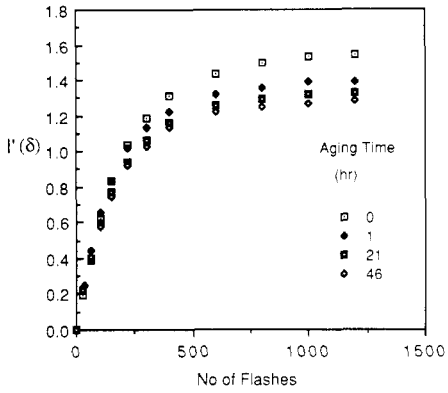

Figure 6. Kinetic plot of photoisomerization of azobenzene group in the chain end labeled polystyrene following cooling from 110 to 80 °C as a function of physical aging time.

sorptions as described earlier. These values of cis isomer content are similar to those reported for azobenzene[23] and its derivatives[24] in dilute solution.

Photoisomerization in Glassy Films. Photoisomerization behavior of the labels in a glassy polystyrene matrix was found to be quite different from the analogous behavior in dilute solution. For comparison with the solution behavior, the representative glassy behavior is illustrated in the bottom of Figures 1–3. One can note clearly by comparing the top spectra with the bottom spectra in Figures 1 and 2 that greater numbers of flashes are needed to induce similar extents of isomerization for the end and side labels. For the center label, isomerization occurs in the glassy state to only a small extent, as shown in Figure 3b. For the free probe, as shown in Figure 4, the glassy state imposes small constraint on the photoisomerization. In spite of differences in the extent of photoisomerization depending on the site of the probe, one common trend was observed: photoisomerization proceeds relatively rapidly at the early stages of conversion but becomes much slower later on. For example, the end label isomerizes by more than 60% after 400 flashes but little more (≈10%) after 1200 further flashes, as illustrated in Figure 1b. In contrast, a photostationary state is reached after only 270 flashes in solution, as shown in Figure 1a. This trend is consistent with our previous findings in glassy polymers where the label was at random locations in the main chain.[15]

Quantitative analyses of the kinetics of photoisomerization based on eq 16 show such trends more clearly, as illustrated in Figure 6 for the end label. Plotted against time in Figure 6 is $I'(\delta)$, which is $I(\delta)$ minus the intercept at $t = 0$. In applying eq 16 to the glassy behavior, we assumed the photostationary fraction of cis isomers, y_∞, to be the same as that in dilute solution, rather than that at the apparent photostationary state in the glass. This is believed to be the more accurate way to analyze the data because the cis isomer content at the apparent photostationary state does continue to increase, even though very slowly, with further irradiation.

We note that in Figure 6 all of the plots are strongly curved, suggesting a combination of fast and slow processes. To estimate the fractions of these processes, we fitted the curves in Figure 6 with

$$e^{-I'(\delta)} = \alpha e^{-A_1 t} + (1 - \alpha)e^{-A_2 t} \qquad (17)$$

where A_1 and A_2 are the rate constants for the fast and slow processes, respectively. Table II summarizes the kinetic parameters (α, A_1, and A_2) based on eq 17 for the end label as a function of physical aging at 80 °C subsequent to cooling from 110 °C as a representative example.

Table II
Kinetic Parameters Based on Eq 17 for Photoisomerization in Glassy State for the End Label

physical aging time, h	α	$10^3 A_1$,[a] s^{-1}	$10^5 A_2$,[b] s^{-1}
0	0.749	6.30	9.23
1	0.717	6.88	8.39
21	0.698	6.16	9.23
46	0.695	6.25	8.81

[a] Experimental errors: less than 10%.

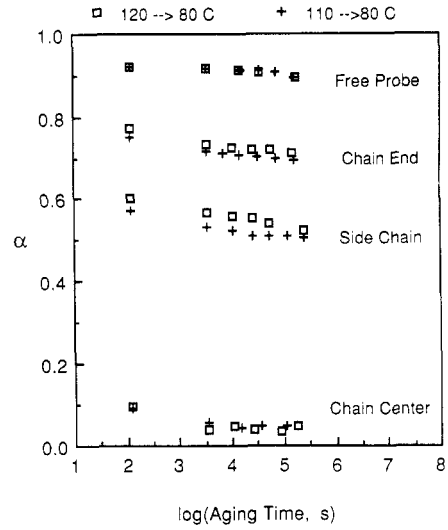

Figure 7. Changes of the fraction of the fast photoisomerization, α, as a function of the physical aging time for the three labeled polystyrenes and the probe in polystyrene (□, following cooling from 120 to 80 °C; +, following cooling from 110 to 80 °C).

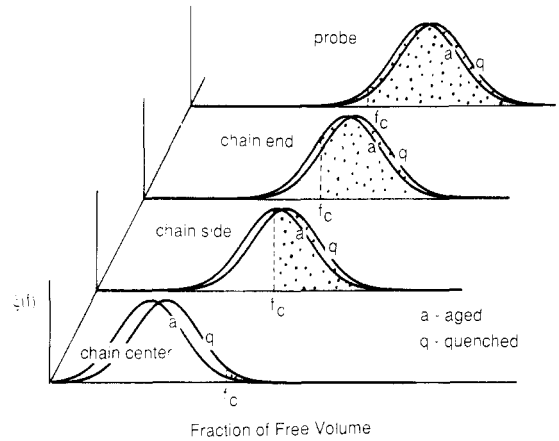

Figure 8. Schematic representation of the distribution of free volume sizes for the three labeled polystyrenes and the probe in polystyrene (line labeled q; after physical aging for 100 s; line labeled a after physical aging for 11 days at 90 °C).

We note from Table II that the values of A_1 and A_2 differ by approximately 2 orders of magnitude and that they remain constant with aging within experimental error. The photoisomerization results from the other labels and the free probe in the polystyrene matrix were also analyzed with eq 17. The values of A_1 and A_2 were found to be of the same order of the magnitude for all the samples, regardless of physical aging history. Moreover, the rate constant for the fast photoisomerization process, A_1, is seen to be about one-third of the rate constant in dilute solution, for the end label.

Figure 7 shows the plot of α as a function of physical aging time at 80 °C for the three labels as well as the free probe in the polystyrene matrix following cooling from 120

Table III
Rate of Physical Aging ($d\alpha/d \log t$) at 80 °C

sample	$10^2\ d\alpha/d \log t$(rate), s^{-1}	
	120 °C → 80 °C	110 °C → 80 °C
P-PS	0.7	0.7
E-PS	1.9	1.7
S-PS	2.2	2.0
C-PS	1.6	1.5

Table IV
Rate of Physical Aging ($d\alpha/d \log t$) after Cooling from 110 °C

sample	$10^2\ d\alpha/d \log t$(rate), s^{-1}	
	90 °C aging temp	70 °C aging temp
P-PS	0.8	0.7
E-PS	1.7	0.8
S-PS	2.7	1.0
C-PS	0.7	1.4

or 110 °C. Since the glass transition temperature of polystyrene is 100 °C, these experiments represent cooling from 20 or 10° above T_g to 20° below. The experimental errors in the magnitudes of these values of α are no more than 0.01 except for the center label. Therefore, all data except for that for the center label are accurate within the sizes of the symbols used in Figure 7. For the center label, the error appears to be greater, about 0.03. The following trends are clearly observed from Figure 7. 1. The α values for the labels and the free probe are in the following decreasing order regardless of the physical aging history: probe > end label > side label > center label. 2. The α values for samples cooled from 120 °C are larger than those for samples cooled from 110 °C for the side and end labels, though the difference is small for the latter. However, there is little difference for the probe and the center label whether they are cooled from 120 or 110 °C. 3. The α values decrease with physical aging time, indicating a shift of the free volume size distribution curve toward smaller sizes. However the rate of decrease of α is in the decreasing order, side > end > center > free probe, as summarized in Table III.

Figure 9 shows the experimental data for α as a function of aging time for three aging temperatures (90, 80, and 70 °C) subsequent to cooling from 110 °C. The following trends can be noted from Figure 9. 1. For the free probe and the center label, the aging temperature does not appear to have much influence on the rate of aging throughout the aging time range studied. 2. The side label exhibits the expected temperature dependence. Aging at 90 °C is the fastest, followed by that at 80 °C and then that at 70 °C. For the end label, aging at 70 °C is again the slowest, but the aging rates at 80 and 90 °C are nearly the same. Table IV summarizes the aging rates estimated from Figure 9; the aging rate data for 80 °C has already been included in the last column of Table III.

Discussion

Mechanism of Photoisomerization. A simple interpretation of the two-process photoisomerization kinetic behavior is that it reflects the distribution of free volume in the glass.[17] Rapid isomerization occurs when the free volume in the vicinity of the label or probe is above a critical amount, and the slow process occurs when the local free volume is below this amount. Unfortunately, the photoisomerization mechanism or mechanisms of the azobenzene labels remain obscure. Not even the mechanism for the thermal cis to trans transition in solution is completely resolved, though it has been studied very extensively.

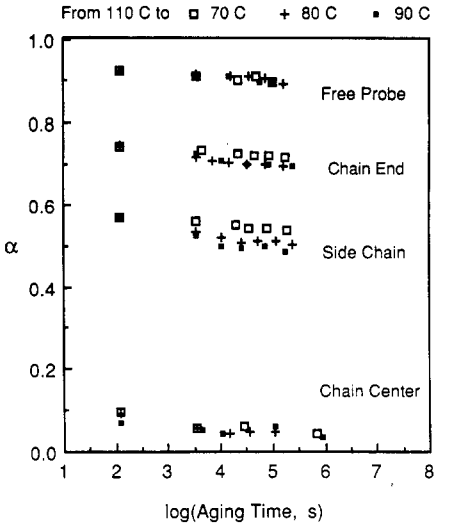

Figure 9. Changes of the fraction of the fast photoisomerization, α, as a function of the physical aging time for the three labeled polystyrenes and the probe in polystyrene, following cooling from 110 °C (■, 90 °C aging; +, 80 °C aging; □, 70 °C aging).

The two mechanisms under consideration for thermal isomerization have been rotation and inversion, the rotation being around the N=N double bond following the rupture of the π-bond and the inversion leaving the π-bond intact. Similar processes are being considered for photoisomerization, with rotation following a $\pi \rightarrow \pi^*$ transition and inversion following an $n \rightarrow \pi^*$ transition.[25] The basis for distinguishing between the two has been through the nature of the transition states, the transition state for rotation being strongly dipolar and that for inversion not.[26] For many azobenzenes under most conditions, the isomerization seems to occur by inversion.[27] Yet the rotational mechanism is still thought to occur in the isomerization of 4-(dimethylamino)-4'-nitroazobenzene, for which the dialkylamino group appears to play the key role.[28] Moreover, there are indications that with certain combinations of solvent and temperature, the mechanism can be made to shift from inversion to rotation with pressure.

The mechanism of isomerization can be expected to be affected by various constraints. Inversion, for instance, is thought to be the only possible mechanism when the azobenzene is constrained by being attached to a ring or across a crown ether.[26,29] The constraint expected for the labels attached to the polymer in bulk polystyrene, though similar, introduces a requirement for coordination of atom movements. If the rearrangement is by inversion, it must be by a roughly symmetrical two-center inversion. On the other hand, rotation about the N–N bond is not precluded by the constraint of the bulk polymer, but a simultaneous rotation about the two adjacent C–N bonds may have to accompany it. Without a detailed computational simulation of the rearrangement, neither of these can be definitely associated with limited free volume. At this point, all that can be said is that photoisomerization seems possible by at least two different mechanisms, and the switch from one mechanism to the other (or another) may be reflected in the dependency of photoisomerization on free volume.

The sharp change in the kinetics at a critical free volume is likely to be more apparent than real. The resolution possible with the experiments described is not very great. Also, kinetic processes are usually very sensitive to free volume. Thus, in any case, from the dominance of one mechanism to that of the other is expected to occur in a

Table V
Parameters for Recovery Kinetics of Polystyrene

$p^* = 7453$ bar[a]	Simha–Somcynsky characteristic parameters
$V^* = 0.9598$ cm^3/g[a]	
$T^* = 12680$ K[a]	
$c_1 = 13.3$[b]	time–temperature shift parameters
$c_2 = 47.5$ K[b]	
$T_g = 373$ K	glass transition temperature
$\tau_g = 1$ h (3600 s)	nominal relaxation time at glass transition
$N_s = 40$	number of segments in recovery region
$z = 12$	size ratio for regions controlling free volume change
$R = 5.3$	translation factor between macroscopic and microscopic processes

[a] Quach, A.; Simha, R *J. Appl. Phys.* **1971**, *42*, 4592. [b] Plazek, D. J. *J. Phys. Chem.* **1965**, *69*, 3480.

narrow range of free volume.

The Labels as Probes of Free Volume. Assuming that the two-process photoisomerization kinetic behavior is related to the distribution of free volume, the fraction of the fast process, σ, can be used to indicate the free volume size distribution in the vicinity of specific sites along the polymer chain or in between the chains as a function of aging time. The fast fraction represents the cumulative area under the free-volume size distribution curve above the critical size. The critical fractional free volume for the photoisomerization of azobenzene was estimated in a previous study to be approximately 0.038, assuming photoisomerization occurs by rotation.[17]

The general trends found for site-specific labels in the glass are illustrated in terms of free volume distribution curves in Figure 8, where a Gaussian function has been assumed for the distribution function. The lines labeled *q* in Figure 8 represent the free volume size distribution curves after 100 s of physical aging at 90 °C; the lines labeled *a* represent the distribution after 100 000 s of physical aging. The shaded areas in Figure 8 show the area under the curve above the critical fractional free volume. The figure shows clearly that for most of the sites occupied by the free probe molecules, the free volume is above the critical size, while most of the sites occupied by the center label are below the critical size. The illustration of these is based on the assumption that the critical free volume is the same for the center label and the free probe. Since the center label is tied at both ends to the polymer chain, one might expect a large critical free volume for the center label, in which case, the free volume distribution would not be skewed as in Figure 8. A comparison of the quenched and aged curves in Figure 8 indicates a significant disappearance of the larger free volume sizes with volume densification (physical aging) for the side and the end labels.

Comparison of Experiment with the RSC Theory. Because the kinetics of photoisomerization in the glassy polystyrene matrix are easily interpreted qualitatively in terms of the free volume distribution in the glass, it is worthwhile testing this interpretation further. This can be done by comparing the change in the population of the rapidly isomerizing sites with predictions from the RSC theory summarized above and given in more detail in ref 18.

The RSC theory has been used to compute the populations of regions having a greater than critical amount of free volume. The parameters for the RSC calculation are given in Table V. They are the same parameters as used previously to fit volume recovery data on polystyrene of Goldbach and Rehage.[18b,30] The regions of interest in the computation are those having the size containing N_s (40, for the present computation) monomer segments. The computation gives the time development of the populations

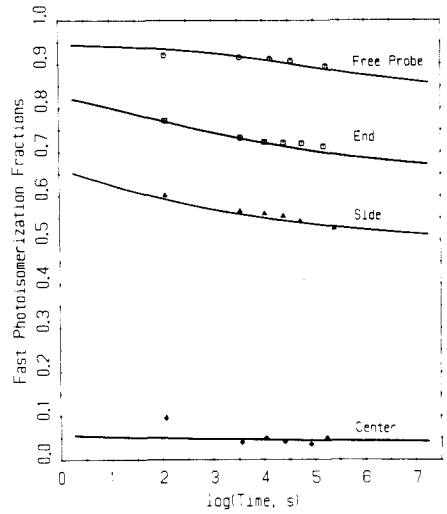

Figure 10. Fast photoisomerization fractions vs annealing time at 80 °C following equilibration at 120 °C. The experimental data are indicated by the points and the prediction is indicated by the solid curves.

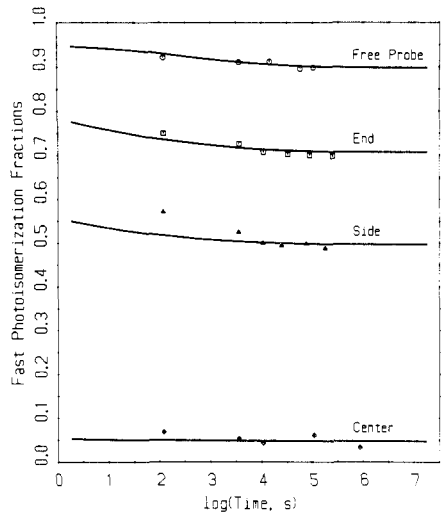

Figure 11. Fast photoisomerization fractions vs annealing time at 90 °C following equilibration at 110 °C. The experimental data are indicated by the points, and the prediction is indicated by the solid curves.

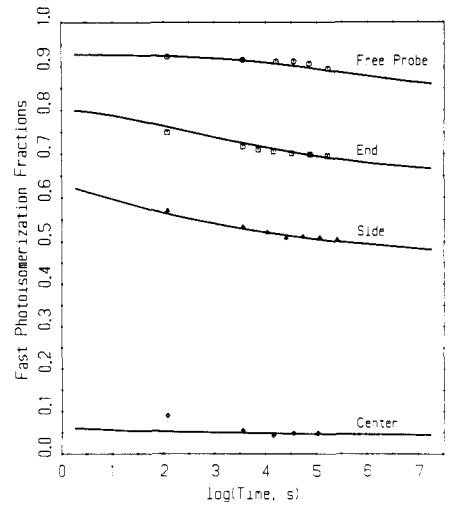

Figure 12. Fast photoisomerization fractions vs annealing time at 80 °C following equilibration at 110 °C. The experimental data are indicated by the points, and the prediction is indicated by the solid curves.

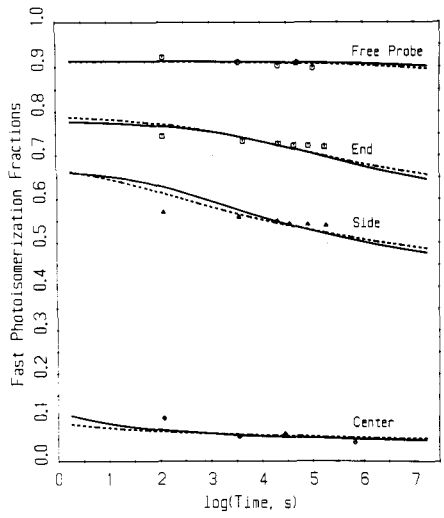

Figure 13. Fast photoisomerization fractions vs annealing time at 70 °C following equilibration at 110 °C. The experimental data is indicated by the points. The prediction of the original RSC theory is indicated by the dashed curves; the predictions of the RSC theory supplemented with the factor in eq 18 with ΔH_g equal to 100 kJ/mol are indicated by the solid curves.

of these regions with various amounts of free volume.

The results of the computation for the fraction of regions having the critical or larger free volume plotted against aging time are shown in Figures 10–13. Represented in these figures are the temperature steps from 120 to 80 °C and from 110 to 90, 80, and 70 °C, respectively. The data for the rapidly isomerizing fractions have been plotted on the same graphs. The theory gives a family of curves and the particular curves here chosen from the family were those that best represent the rapidly isomerizing fractions for each azobenzene location.

The main lack of correspondence between theory and experiment is with the 70 °C data in Figure 13. (The points in Figures 10–13 closest to the ordinate, those just above 100 s, were not aged at the temperatures indicated but were obtained by quenching from the initial temperature to room temperature. Thus, their lack of fit by the computed curves, especially in Figures 11 and 13, is of little concerned.) The fast photoisomerization fractions at longer times in Figure 13 are seen to change more slowly with time than predicted. This problem with the theory, arising from a large downward step in temperature, had been noted earlier.[31] It is believed to arise from an inadequate account being taken by the theory of thermal effects. An improvement in the theory had been obtained previously by using in the free volume step rate in eq 10 an extra Arrhenius factor of the following form[31,32]

$$F = \exp[(1 - \theta/T)\Delta H_g/RT_g] \tag{18}$$

where θ is a fictive temperature descriptive of the structure, T is the actual temperature, and ΔH_g is the incremental activation energy at the conventional glass transition temperature T_g. In equilibrium, when $\theta = T$, the entire factor becomes unity and has no effect. The need for some such factor in the glass is that the WLF equation, which is used in eq 10 to convert free volume to a rate, depends on only a single variable, either free volume, as here, or temperature. Yet the effects of both thermal agitation and structure in the liquid need to be accounted for. Although previous supplementation of the free volume theory by the Arrhenius term in eq 18 had been successful,[31-33] its use in Figure 13 is much less so. The original RSC theory yields the dashed curves: the theory supplemented by the above Arrhenius term with ΔH_g equal to 100 kJ/mol yields the solid curves. The Arrhenius term moves the inflection in the curves to longer times, but the problem in Figure 13 is that it has moved the inflection into the time region of the experiments, which degrades the fit. To move the inflection to times well beyond those of the experiments would require an unrealistically large activation enthalpy, however. The comparison between theory and experiment in Figure 13 indicates that a better theory than that implicit in the factor in eq 18 is needed.

Except for the recovery data at 70 °C, the computed fit to the data is quite satisfactory. Moreover, the aspect of the RSC theory being tested is in some respects its uniqueness with respects to other aging theories, its reliance on a distribution of free volume, which is assumed to be generated by thermal fluctuations. Thus, with the assumption that the fast and slow photoisomerization processes do in fact arise from different amounts of free volume, as seems likely, then these experiments yield directly the distribution of free volume. Furthermore, the distribution it yields seems to be exactly that predicted.

Interpretation of the Free Probe Experiments. A question of some interest is whether the free probe represents a measure of the average free volume in the matrix. On the basis of the above experimental results, the answer to this question seems to be no; the free probe appears to be associated with much larger free volume sizes. This conclusion is reached from the results in Figures 7 and 9. If the free probe were reflecting the average free volume, it would be expected to reflect a value falling between those of the end and center labels and close to that of the side label. Instead, the values of α for the probe were always greater than that for the end-label.

In addition to this qualitative argument, we can offer more quantitative support for this question by using the free volume distribution described by the γ function.[7b] This is given by

$$\xi(f) = [\lambda/\Gamma(\alpha)](\lambda f)^{\alpha-1}e^{-\lambda f} \tag{19}$$

where ξ is the size distribution function, f is the fractional free volume, and α and λ are the characteristic material parameters given by

$$\alpha = \langle f \rangle \lambda \tag{20}$$
$$\lambda = \langle f \rangle V/\Delta\kappa kT$$

where $\langle f \rangle$ is the mean fractional free volume, $\Delta\kappa$ is the difference in compressibility between the liquid and glass, k is the Boltzmann constant, T is the temperature, and V is the volume of the relaxation environment. We have estimated V and the critical fractional free volume for the azobenzene species to be 4.96 nm^3 and 0.038, respectively, assuming a rotation for the photoisomerization mechanism.[17] Using the values of 2.5×10^{-10} Pa^{-1} for $\Delta\kappa$ near T_g[34] and 0.028 for $\langle f \rangle$ at T_g,[35] we estimate α and λ to be 4.63 and 165.53, respectively, at 80 °C.

The free volume distribution function at 20 °C for polystyrene has been calculated, in the same way as described in ref 17. The area above $f_{cr} = 0.038$ has been measured to about 20% of the total area. This value would be the expected average a value from the experiment if the probe represents the average free volume. The fact that the a values for the probe are much greater than predicted clearly suggests that this particular probe in a polystyrene matrix does not sample the average environment.

This should not, perhaps, be a surprising result. The free probe, being free, is expected on thermodynamic grounds to seek our regions in the bulk with the greatest free volume. This would maximize the entropy. The only exception would be if there were a specific interaction with the polymer, for which the free energy of the system would

be minimized by the free probe not seeking regions of maximum free volume. But this seems not to be the case with the azobenzene probe employed and polystyrene.

Acknowledgment. W. C. Yu and C. S. P. Sung wish to acknowledge the financial support for this work from the National Science Foundation, Polymers Program (Grant No. DMR 82-05897), and the Army Research Office (Contract No. DAA 29-85-K-0055).

Registry No. 4-$H_2NC_6H_4N{=}NC_6H_5$, 60-09-3.

References and Notes

(1) Struik, L. C. E. *Physical Aging in Amorphous Polymers and Other Materials*: Elsevier, New York, 1978.
(2) Petrie, S. E. B. *J. Polym. Sci., Part A-2* **1972**, *10*, 1255.
(3) Petrie, S. E. B. *Physical Structure of the Amorphous State*; Allen, G., Petrie, S. E. B., Eds.; Marcel Dekker: New York, 1976; p 225.
(4) Levita, G.; Smith, T. L. *Polym. Eng. Sci.* **1981**, *21*, 936.
(5) Roe, R. J.; Millman, G. M. *Polym. Eng. Sci.* **1983**, *23*, 318.
(6) (a) Wendorff, J. H. *J. Polym. Sci., Polym. Lett. Ed.* **1979**, *17*, 765. (b) Roe, R. J.; Curro, J. J. *Macromolecules* **1983**, *16*, 428. (c) Roe, R. J., private communication, 1987.
(7) (a) Cohen, M. H.; Turnbull, D. *J. Chem. Phys.* **1959**, *31*, 1164. (b) Robertson, R. E. *J. Polym. Sci., Polym. Symp.* **1978**, *63*, 173. (c) Curro, J. G.; Lagasse, R. R.; Simha, R. *Macromolecules* **1982**, *15*, 1621. (d) Jain, S. C.; Simha, R. *Macromolecules* **1982**, *15*, 1522.
(8) (a) Robertson, R. E. *J. Polym. Sci., Polym. Phys. Ed.* **1979**, *17*, 597. (b) Robertson, R. E. *Ann. N.Y. Acad. Sci.* **1981**, *371*, 21.
(9) (a) Curro, J. J.; Roe, R. J. *Polymer* **1984**, *25*, 1424. (b) Roe, R. J.; Song, H. H. *Macromolecules* **1985**, *18*, 1603.
(10) (a) Ache, H., Ed. *Positronium and Muonium Chemistry*; Advances in Chemistry 175; American Chemical Society: Washington, DC, 1979. (b) Siegel, R. W. *Annu. Rev. Mater. Sci.* **1980**, *10*, 393.
(11) Eldrup, M. In *Positron Annihilation*; Coleman, P. G., Sharma, S. C., Diana, L. M., Eds.; North-Holland: Amsterdam, 1982; p 753.
(12) Jean, Y. C.; Sandrecki, T. C.; Ames, D. P. *J. Polym. Sci., Polym. Phys. Ed.* **1986**, *24*, 1247.
(13) Ujihara, Y.; Ryuo, T.; Kobayashi, Y.; Nomizu, T. *Appl. Phys.* **1978**, *16*, 71.
(14) (a) Malhortra, B. D.; Pethrick, R. A. *Eur. Polym. J.* **1983**, *19*, 457. (b) Malhortra, B. D.; Pethrick, R. A. *Polymer* **1983**, *24*, 165.
(15) Lamarre, L.; Sung, C. S. P. *Macromolecules* **1983**, *16*, 1729.
(16) Tsay, F. D.; Hong, S. D.; Moacanin, J.; Gupta, A. *J. Polym. Sci., Polym. Phys. Ed.* **1982**, *20*, 763.
(17) Sung, C. S. P.; Gould, I. R.; Turro, N. J. *Macromolecules* **1984**, *17*, 1447.
(18) (a) Robertson, R. E.; Simha, R.; Curro, J. G. *Macromolecules* **1984**, *17*, 911. (b) Robertson, R. E.; Simha, R.; Curro, J. G. *Macromolecules* **1985**, *18*, 2239.
(19) Law, K. L.; Loutfy, R. O. *Macromolecules* **1981**, *14*, 587.
(20) Simha, R.; Somcynsky, T. *Macromolecules* **1969**, *2*, 342.
(21) Curro, J. G. *J. Macromol. Sci., Rev. Macromol. Chem.* **1974**, *C11*, 321.
(22) Cox, D. R.; Miller, H. D. *The Theory of Stochastic Processes*; Chapman and Hall: London, 1965, Chapter 4.
(23) (a) Zimmerman, G.; Chow, L.; Paik, U. *J. Am. Chem. Soc.* **1958**, *80*, 3528. (b) Victor, J. G.; Torkelson, J. M. *Polym. Prepr. (Am. Chem. Soc., Div. Polym. Sci.)* **1986**, *54*(1), 700.
(24) Priest, W. J.; Sifain, M. M. *J. Polym. Sci., Polym. Chem. Ed.* **1971**, *9*, 3161.
(25) Rau, H. *J. Photochem.* **1984**, *26*, 221.
(26) Schanze, K. S.; Mattox, T. F.; Whitten, D. G. *J. Org. Chem.* **1983**, *48*, 2808.
(27) (a) Otruba, J. P.; Weiss, R. G. *J. Org. Chem.* **1983**, *48*, 3448. (b) Marcandalli, B.; Pellicciari-Di Liddo, L.; Di Fede, C.; Bellobono, I. R. *J. Chem. Soc., Perkin Trans. 2* **1984**, 589. (c) Nishimura, N.; Tanaka, T.; Sueishi, Y. *J. Chem. Soc., Chem. Commun.* **1985**, *903*.
(28) (a) Asano, T.; Yano, T.; Okada, T. *J. Am. Chem. Soc.* **1982**, *104*, 4900. (b) Asano, T.; Okada, T. *J. Org. Chem.* **1984**, *49*, 4387.
(29) (a) Shinkai, S.; Kusano, Y.; Shigematsu, K.; Manabe, O. *Chem. Lett.* **1980**, 1303. (b) Asano, T.; Okada, T.; Shinkai, S.; Shigematsu, K.; Kusano, Y.; Manabe, O. *J. Am. Chem. Soc.* **1981**, *103*, 5161. (c) Rau, H.; Luddecke, E. *J. Am. Chem. Soc.* **1982**, *104*, 1616.
(30) Goldbach, G.; Rehage, G. *J. Polym. Sci., Part C* **1967**, *16*, 2289.
(31) Robertson, R. E.; Simha, R.; Curro, J. G., to be submitted for publication.
(32) Robertson, R. E. *J. Appl. Phys.* **1978**, *49*, 5048.
(33) Matsuoka, S.; Williams, G.; Johnson, G. E.; Anderson, E. W.; Furukawa, T. *Macromolecules* **1985**, *18*, 2652.
(34) Goldbach, G.; Rehage, G. *Rheol. Acta* **1967**, *6*, 30.
(35) Plazek, D. J. *J. Phys. Chem.* **1965**, *69*, 3480.